Silica-Immobilized Zinc β-Diiminate Catalysts for the Copolymerization of Epoxides and Carbon Dioxide

Kunquan Yu and Christopher W. Jones*

School of Chemical Engineering, Georgia Institute of Technology, 311 Ferst Drive, Atlanta, Georgia 30332

Received March 19, 2003

A synthetic protocol has been developed to prepare silica-supported Zn−β-diiminate catalysts for the copolymerization of cyclohexene oxide (CHO) and CO_2. Multiple strategies have been developed for the immobilization of these β-diiminate zinc complexes onto the surface of model silica materials such as mesoporous SBA-15 and controlled-pore glass (CPG). The β-diiminate ligand has been modified to incorporate a C═C double bond or an alkane spacer with a trimethoxysilyl end group, allowing immobilization via direct reaction of the alkoxysilanes with silanols on the surface or via AIBN-promoted C═C bond coupling with thiol-functionalized silica. The immobilization process has been followed using FT-Raman spectroscopy and thermogravimetric analysis, whereas polymers have been characterized by GPC and NMR. The resulting silica-supported catalysts exhibit good activity in the alternating copolymerization of CHO and CO_2, leading to polymers with varying degrees of carbonate linkages (copolymerization) relative to ether linkages (homopolymerization of epoxide). Immobilizing the complexes on the silica support leads to catalysts that give more polymeric ether linkages than their corresponding homogeneous analogues. Control studies indicate that this is due, at least in part, to starvation of the active site of CO_2, especially at later stages of the polymerization.

Introduction

The immobilization of homogeneous catalysts to facilitate easy product separation, catalyst recovery, and recycling constitutes a well-established research area in small-molecule catalysis. In contrast, it is significantly less common in polymerization catalysis.[1] Catalyst recovery and recycling in polymerization reactions is exceedingly rare, yet a technology that would potentially allow recovery could have important benefits, such as allowing the preparation of metal-free polymers for biomedical applications. Similarly, such a technology could make systems that utilize expensive catalysts of relatively low activity commercially attractive. To this end, in our laboratories, we are investigating potential strategies for the preparation of recoverable and recyclable polymerization catalysts.

There are several issues that make the design of recoverable polymerization catalysts different from, and generally more difficult than, the design of corresponding small-molecule catalysts. In small-molecule reactions (e.g. hydrogenation of simple olefins) on solid catalysts, the catalytic process involves diffusion of the reactants to the active site, binding at the active site, progression through the various steps of the catalytic cycle, and then desorption from the active site and diffusion away from the solid catalyst. In polymerization catalysis, most of these steps are the same, with the exception of transport of the reactants to the active site and the products away from the active site. Because the product of the reaction is a polymer that has a substantially lower diffusion coefficient than typical small molecules (and because the polymer remains attached to the catalyst in coordination−insertion catalysts), the area around the catalytic active site can be a very dynamic environment due to the inability of the polymer to effectively move away from the site. If a porous catalyst is used, at the outset of the reaction, the reaction will usually be kinetically limited. However, as time progresses, the pores of the catalyst can fill with polymer, the process can enter a diffusion-limited regime, and the overall rate of polymerization can be significantly retarded. Two key issues arise as a result of this: (1) the kinetics of the reaction become complex and more difficult to analyze, and (2) the recovery of the catalyst after reaction can become impossible if the sparingly soluble or completely insoluble polymer engulfs the pores of the catalyst. Hence, in the design of catalysts for polymerization reactions when catalyst recovery is desired, both the design of the active site and the design of the catalyst pore structure must be considered simultaneously. In particular, the following three factors are critically important: (1) when a single-site, homogeneous catalyst is immobilized, extreme care must be taken to develop a synthetic protocol that gives a solid catalyst with a single type of site, (2) the support pore structure must be amenable to facile transport of reactants to the active sites and polymers away from the sites, and (3) when the reaction is quenched, the active site must not be altered (quenching the reaction

* To whom correspondence should be addressed. E-mail: cjones@che.gatech.edu. Tel: 404-385-1683.

(1) Homogeneous catalysts such as metallocenes are routinely immobilized for α-olefin polymerizations, but the catalysts are not recovered.

10.1021/om030209w CCC: $25.00
Publication on Web 05/22/2003

cannot decompose the catalyst) if the catalyst is meant to be recycled. Hence, the design of supported, recoverable polymerization catalysts is a very complex process with demanding requirements.

Inoue first reported the alternating copolymerization of carbon dioxide and epoxide using $ZnEt_2$ and H_2O in 1969.[2] Since then, a variety of other zinc complexes have been investigated for this copolymerization process.[3−10] We have identified the work of Coates and co-workers on well-defined β-diiminate (BDI) zinc complexes for the alternating copolymerization of cyclohexene oxide (CHO) and CO_2 as potential catalysts for our initial studies of recoverable polymerization catalysts.[9] These well-defined zinc catalysts are among the first catalysts reported for the living synthesis of high-molecular-weight polymer from epoxides and CO_2. The catalysts display high activity under mild conditions and are single-site in nature. The fact that copolymerizations using these catalysts can be quenched using simple alcohols and that the initiating group on the catalyst can be an alkoxy species gave some hope to the possibility that such a supported catalyst could be effectively recycled.

In this work, we report our initial investigations into the design of recoverable and potentially recyclable supported polymerization catalysts. Modified zinc β-diiminate complexes can be easily immobilized on silica supports such as mesoporous SBA-15[11] and controlled-pore glass (CPG). The resulting solid-supported system exhibits good activity for the copolymerization of CHO and CO_2 and offers a potential way for catalyst separation and recycling. Here we report the detailed synthesis and characterization of the silica-supported catalyst, and the composition of the produced polycarbonate is related to the synthetic protocol employed.

Scheme 1

Immobilization Position 1 Immobilization Position 2

Results and Discussion

Syntheses and Spectroscopic Studies. Two potential ligand modifications were envisioned that could potentially be used to facilitate binding the zinc BDI complex to a silica surface. Both involved modification of the BDI ligand at locations that would likely prevent detrimental effects on the activity and selectivity of the catalyst. These locations were off the terminal methyl group on the dione precursor and para to the nitrogen on the aromatic ligand (Scheme 1). Protocols were developed to add terminal olefins in these locations.

For functionalization on the dione precursor, the reaction of allyl bromide with the dianion of 2,4-pentanedione was utilized to afford the ligand precursor for (BDI-1)H. This precursor was then reacted with 2 equiv of 2,6-diisopropylaniline in acidic ethanol followed by neutralization with saturated sodium carbonate to give the ligand (BDI-1)H (Scheme 2a). In the other approach, reacting allyl chloride with 2,6-diisopropylaniline followed by an aza-Claisen rearrangement afforded the allyl-modified aniline. Further reaction with 0.5 equiv of 2,4-pentanedione gave (BDI-2)H (Scheme 2b). The $ZnCl_2$-catalyzed aza-Claisen rearrangement always resulted in a mixture of *N*-allyl- and 4-allyl-2,6-diisopropylaniline. Although separation can be accomplished by careful vacuum distillation, yields were low, with an overall yield for (BDI-2)H of only 18%. The final ligand employed, (BDI-1-MPTS)H, was prepared in a quantitative yield by utilizing an AIBN-initiated coupling reaction between the C═C double bond and the −SH group (Scheme 3).[12]

Diethylzinc reacts with the β-diimine ligands in quantitative yields to produce (BDI-1)ZnEt, (BDI-2)-ZnEt, and (BDI-1-MPTS)ZnEt (Scheme 3) and afford the corresponding methoxide complexes in high yields after treatment with 1 equiv of methanol.[9a] However, treatment of the zinc amide complex with 1 equiv of 2-propanol gave zinc isoproxides in poor to moderate yields (56%) after recrystallization from toluene at −30 °C. In the case of (BDI-1-MPTS)ZnN$(SiMe_3)_2$, 4 equiv of alcohol was used, since 2-propanol also reacts with the trimethoxy group, though it is unlikely that it would displace all three −OMe groups due to steric constraints (proton NMR indicates a mono displacement). Whereas for $[(BDI\text{-}1)ZnOMe]_2$ the syn/anti ratio of the complex is ∼1:3 by proton NMR, the ^1H NMR spectra of both the methyl and isopropyl BDI-1-MPTS−Zn−alkoxy complexes show only one set of peaks. This presumably suggests that only the anti arrangement exists in the solution, due to the steric bulkiness of the ligand. Note that the coupling of the organosilane to the modified BDI ligands was carried out using the reaction of the

(2) Inoue, S.; Koinuma, H.; Tsuruta, T. *J. Polym. Sci., Part B: Polym. Lett.* **1969**, *7*, 287−292.

(3) For reviews on epoxide/CO_2 copolymerization, see: (a) Darensbourg, D. J.; Holtcamp *Coord. Chem. Rev.* **1996**, *153*, 155−174. (b) Super, M. S.; Beckman *Trends Polym. Sci.* **1997**, *5*, 236−240. (c) Rokicki, A.; Kuran, W. *J. Macromol. Sci. Rev. Macromol. Chem. Phys.* **1981**, *C21*, 135−186.

(4) (a) Darensbourg, D. J.; Wildeson, J. R.; Yarbrough, J. C. *Inorg. Chem.* **2002**, *41*, 973−980. (b) Darensbourg, D. J.; Adams, M. J.; Yarbrough, J. C. *Inorg. Chem.* **2001**, *40*, 6543−6544. (c) Darensbourg, D. J.; Rainey, P.; Yarbrough, J. *Inorg. Chem.* **2001**, *40*, 986−993. (d) Darensbourg, D. J.; Zimmer, M. S.; Rainey, P.; Larkins, D. L. *Inorg. Chem.* **2000**, *39*, 1578−1585. (e) Darensbourg, D. J.; Wildeson, J. R.; Yarbrough, J. C.; Reibenspies, J. H. *J. Am. Chem. Soc.* **2000**, *122*, 12487−12496. (f) Darensbourg, D. J.; Holtcamp, M. W.; Struck, G. E.; Zimmer, M. S.; Niezgoda, S. A.; Rainey, P.; Robertson, J. B.; Draper, J. D.; Reibenspies, J. H. *J. Am. Chem. Soc.* **1999**, *121*, 107−116. (g) Darensbourg, D. J.; Holtcamp, M. W. *Macromolecules* **1995**, *28*, 7577−7579.

(5) Sârbu, T.; Beckman, E. J. *Macromolecules* **1999**, *32*, 6904−6912.

(6) (a) Nozaki, K.; Nakano, K.; Hiyama, T. *J. Am. Chem. Soc.* **1999**, *121*, 11008−11009. (b) Nakano, K.; Nozaki, K.; Hiyama, T. *J. Am. Chem. Soc.*, in press.

(7) Dinger, M. B.; Scott, M. J. *Inorg. Chem.* **2001**, *40*, 1029−1036.

(8) Chisholm, M. H.; Navarro-Llobet, D.; Zhou, Z. *Macromolecules* **2002**, *35*, 6494−6504.

(9) (a) Cheng, M.; Moore, D. R.; Reczek, J. J.; Chamberlain, B. M.; Lobkovsky, E. B.; Coates, G. W. *J. Am. Chem. Soc.* **2001**, *123*, 8738−8749. (b) Cheng, M.; Lobkovsky, B. M.; Coates, G. W. *J. Am. Chem. Soc.* **1998**, *120*, 11018−11019. (c) Cheng, M.; Darling, N. A.; Lobkovsky, E. B.; Coates, G. W. *Chem. Commun.* **2000**, 2007−2008.

(10) (a) Chisholm, M. H.; Gallucci, J.; Phomphrai, K. *Inorg. Chem.* **2002**, *41*, 2785−2794. (b) Chisholm, M. H.; Huffman, J. C.; Phomphrai, K. *J. Chem. Soc., Dalton Trans.* **2001**, 222−224.

(11) (a) Zhao, D.; Feng, J.; Hou, Q.; Melosh, N.; Fredrickson, G. H.; Chmelka, B. F.; Stucky, G. D. *Science* **1998**, *279*, 548. (b) Zhao, D.; Hou, Q.; Feng, J.; Chmelka, B. F.; Stucky, G. D. *J. Am. Chem. Soc.* **1998**, *120*, 6024−6036.

(12) Burger, H.; Sawodny, W.; Wannagat, U. *J. Organomet. Chem.* **1965**, *3*, 113−120.

Scheme 2

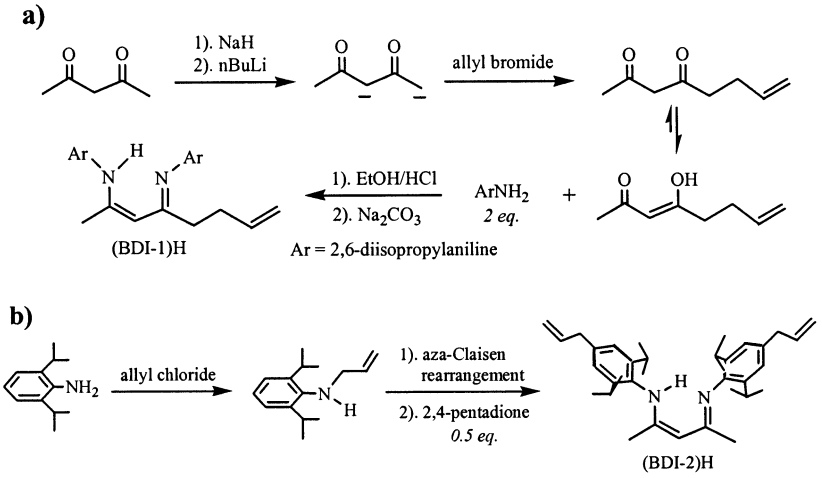

Scheme 3

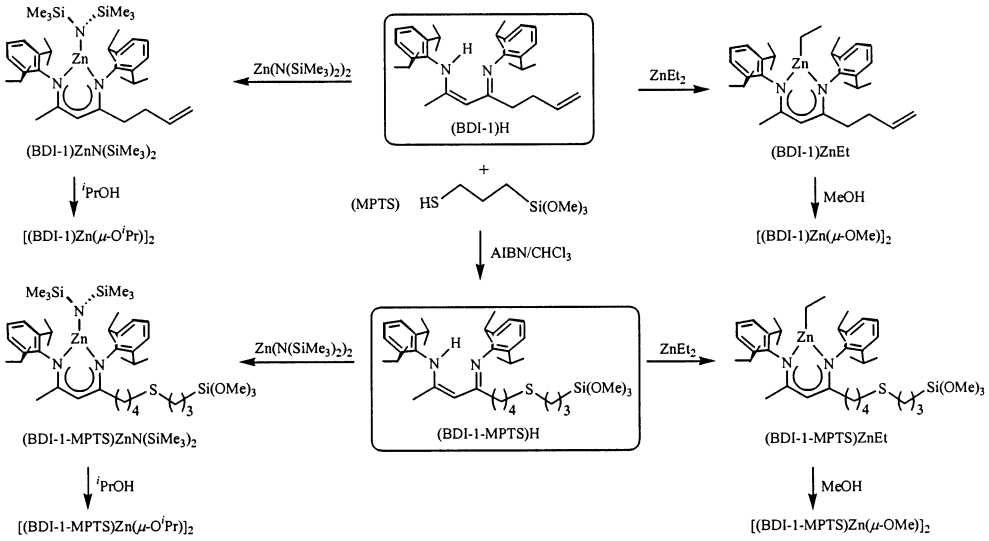

terminal olefin with a thiol, because more traditional approaches such as hydrosilylation of the terminal olefins gave either no product or very low yields, presumably due to binding of the platinum hydrosilylation catalyst by the uncomplexed BDI ligands.

Immobilization on the Silica Surface. Two different silica materials with different pore sizes and pore connectivities were used as hosts for the zinc catalysts. SBA-15 is a well-defined hexagonal mesoporous silica material with straight mesopores that are connected through small micropores.[11] The SBA-15 used in this study has an average mesopore size of 105 Å and a surface area of 830 m^2/g on the basis of low-temperature N_2 physisorption measurements. Hexagonal mesoporous silicas of this type are useful model supports because they have well-defined, tailorable mesopore systems with little polydispersity. This well-defined pore system will facillitate quantitative kinetic analysis of the transition between kinetic and diffusive regimes in these catalysts, a potential topic of future investigation. However, for industrial application and maximization of reaction rates, these supports are not optimal due to the unidimensional nature of the pores.

For this reason, a different silica material with larger, interconnected pores was also studied. This second silica material that was employed is controlled-pore glass (CPG), a lower surface area (~80 m^2/g), mesoporous solid with an average pore size of 246 Å and a narrow pore size distribution. This material has pores that are interconnected randomly. Because of the sensitivity of the zinc complexes toward water, the calcined silica materials SBA-15 and CPG-246 were fully dried under high vacuum, first at room temperature overnight and then at 120 °C for 3 h. The surface silanol content[13] for SBA-15 determined by TGA is approximately 4.0 mmol/g of silica, whereas for CPG, it is only about 1.0 mmol/g of silica.

Three different methods were explored for the immobilization of the zinc complexes onto the silica surface.

(a) Method 1 (Scheme 4). This method was based on a direct reaction of the trimethoxysilyl group of metalated BDI-1-MPTS with surface silanols to form a Si−O−Si bond with concomitant release of methanol.

(13) Based on the condensation reaction of two Si−OH groups in forming a Si−O−Si bond with concomitant release of a H_2O molecule. This approach assumes that all silanol groups are surface groups that all are accessible for functionalization. A more quantitative method to determine the silanol content was described in: (a) Fujdala, K. L.; Tilley, T. D. *J. Am. Chem. Soc.* **2001**, *123*, 10133−10134. (b) Rice, G. L.; Scott, S. L. *Langmuir* **1997**, *13*, 1545.

Scheme 4. Method 1

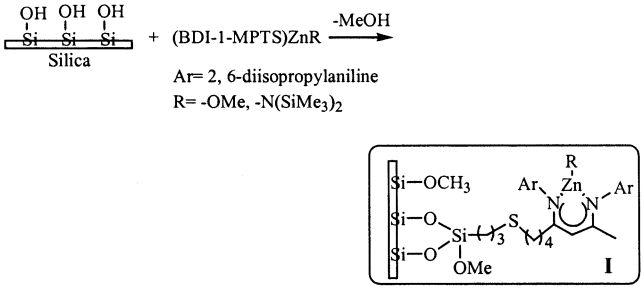

Scheme 5. Method 2

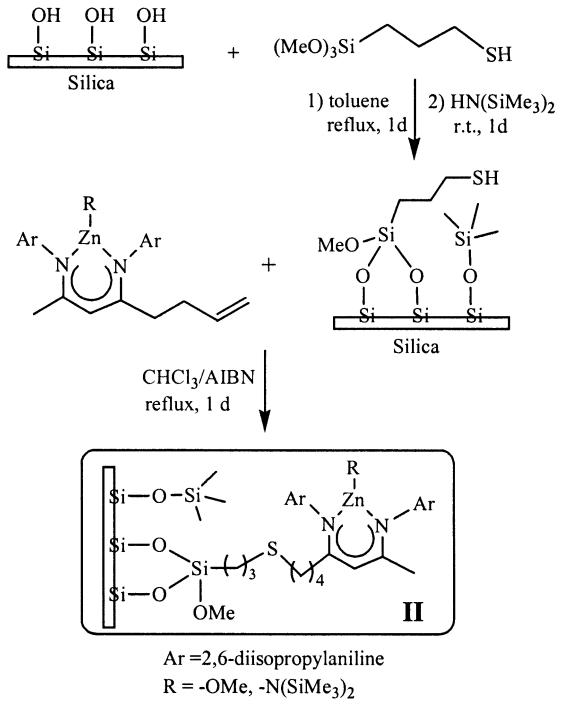

This method is the most straightforward one, and the only real concern is whether the surface silanols will interact with the zinc metal center.

(b) Method 2 (Scheme 5). Method 2 was based on a coupling reaction between the double bond and a thiol group, the same reaction used to prepare (BDI-1-MPTS)H (Scheme 3). However, in this case, the thiol group was first immobilized on silica and then the olefin-terminated metal complex was reacted with the functionalized silica. Thiol-functionalized SBA-15 was prepared by refluxing with excess (3-mercaptopropyl)-trimethoxysilane (MTPS) in a toluene solution for 24 h and recovering by filtration with toluene washing in a drybox. Capping the remaining surface silanols was achieved by further reacting at room temperature with hexamethyldisilazane in toluene. Following this capping treatment, the thiol-functionalized SBA-15 was dried under vacuum overnight at room temperature. Using this method, potential interactions between zinc and the silanols on the silica surface are strongly reduced, due to the coverage of the silica surface with thiol and $-SiMe_3$ groups. However, interactions between the acidic thiol species and the zinc metal center are possible. This issue will be addressed in a subsequent section.

The immobilization through method 2 was characterized by FT-Raman spectroscopy (Figure 1). The spectrum for thiol-functionalized SBA-15 shows a peak around 2577 cm^{-1}, characteristic of the S−H stretching. FT-Raman spectra of $[(BDI\text{-}1)ZnOMe]_2$ showed two peaks at 1662 and 1641 cm^{-1} for the cis and trans configurations, respectively, of the C=C bond in the ligand.[14] The disappearance of the thiol and double-bond stretching after the coupling reaction was apparent in Figure 1C. The existence of the aromatic C−H stretching at 3058 cm^{-1} further supports that the β-diiminate ligand is incorporated in the solid catalysts. The decreased intensity was due to the low concentration of the β-diiminate ligand on the silica surface. Due to sample fluorescence, we were not able to observe the Zn−O and Zn−N stretching.

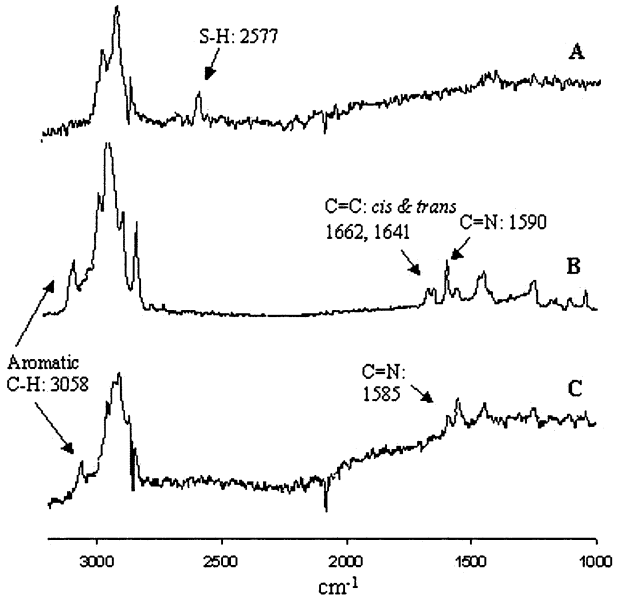

Figure 1. FT-Raman spectra: (A) SBA-15-SH-Capped; (B) $[(BDI\text{-}1)ZnOMe]_2$; (C) species after $[(BDI\text{-}1)ZnOMe]_2$ was immobilized on the thiol-functionalized SBA-15. Raman samples were prepared in a drybox with ~20 mg of the solid sample placed into a J. Young Raman tube for analysis under dry N_2.

Scheme 6. Method 3

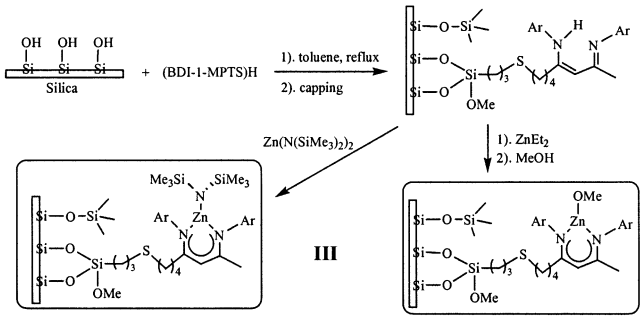

(c) Method 3 (Scheme 6). In this method, the silica surface is first functionalized with the ligand and, subsequently, the immobilized ligand is metalated. For example, the (BDI-1-MPTS)H ligand can be immobilized on the silica surface to afford the surface-silanol-free β-diiminate-functionalized silica after capping with

(14) The two BDI-1 ligands in $[(BDI\text{-}1)Zn(\mu\text{-}OMe)]_2$ adopted cis and trans configurations; for C=C stretching frequencies in Raman see: Bowen, R. D.; Edwards, H. G. M.; Farwell, D. W.; Rusike, I.; Saunders, D. M. *J. Chem. Res.,Synop.* **1998**, 426−427. *J. Chem. Res., Miniprint* **1998**, 1901−1918.

Table 1. Catalytic Results for the Copolymerization of CHO and CO_2[a]

entry	complex	TON	TOF	carbonate linkages (%)[b]	M_n (kg/mol)	M_w/M_n[c]
1	$[(BDI)ZnOMe]_2$	370	185	98	15.2	1.04
2	$[(BDI\text{-}1)ZnOMe]_2$	220	110	96	11.1	1.03
3	$(BDI\text{-}1)ZnN(SiMe_3)_2$	160	80	91	18.2	1.10
4	$[(BDI\text{-}1)ZnO^iPr]_2$	216	108	95	13.4	1.06
5	$[(BDI\text{-}2)ZnOMe]_2$	140	70	98	9.7	1.04
6	$(BDI\text{-}2)ZnN(SiMe_3)_2$	125	62	93	14.6	1.09
7	$[(BDI\text{-}2)ZnO^iPr]_2$	132	66	95	12.1	1.07
8	$[(BDI\text{-}1\text{-}MPTS)ZnOMe]_2$	120	60	98	8.7	1.28
9	$(BDI\text{-}1\text{-}MPTS)ZnN(SiMe_3)_2$	130	65	92	13.3	1.09

[a] All reactions were performed in neat CHO with a monomer-to-zinc ratio of 1000:1 at 50 °C for 2 h with a constant CO_2 pressure of 100 psi. The turnover number (TON) is given in moles of CHO consumed per mole of zinc, assuming all zinc sites are active; the turnover frequency (TOF) is given in moles of CHO consumed per mole of zinc per hour (thus, this is a lower bound on the TOF, as the catalyst may not be active for the full 2 h and perhaps not all zinc sites participate in the reactions). [b] Calculated by integration of methine resonances in ^1H NMR of the polymer; estimated error is ±0.5%. [c] The polymer was characterized with GPC using polystyrene standards in THF.

hexamethyldisilazane. Following this step, solid-supported catalysts can be made by heterogeneous metalation with a zinc source. This process, however, likely gives the least defined catalyst geometry among the three methods. The quantitative preparation of the homogeneous complex (BDI-1-MPTS)ZnEt indicates that diethylzinc will not react with the Si−OMe bond. Furthermore, it has been reported that dimethylzinc caused insignificant or no damage to the framework of dry silica and chlorinated silica as well as trimethylsilyl-capped silica.[15] Thus, it is unlikely that that diethylzinc will interact with the framework of the trimethylsilyl-capped β-diiminate-functionalized silica and metalation of the surface-bound ligand should proceed. However, the ethyl form of the complex needs to be converted to an alkoxy form for the complex to initiate the polymerization. It is not clear if there was a complete conversion of Zn−Et to Zn−OMe upon treatment with methanol, since methanol can also react with the silica surface. Elemental analysis of the nitrogen and zinc content of the as-prepared III−ZnOMe showed a N:Zn molar ratio of 1.67, very close to the theoretical value of 2, but it is unclear if all or most of the zinc is still complexed with the BDI ligand, as excess methanol can demetalate the ligand. Unfortunately, neither NMR nor FT-Raman spectroscopic methods could shed light on Zn coordination. It is believed that incomplete conversion to the metal alkoxide may well account for the low activity (vide infra) of the catalyst prepared from this method.

Copolymerization of Cyclohexene Oxide and Carbon Dioxide. A variety of modified zinc β-diiminate complexes were investigated for the copolymerization of CHO and CO_2 under the same conditions used by Coates,[9a] and the polymerization results are summarized in Table 1. Our catalytic reaction protocol was checked using Coates' original $[(BDI)ZnOMe]_2$, and our observations were very consistent with those reported by Coates.[9a] Previous mechanistic studies[9] involving $[(BDI)ZnOR]_2$ revealed that subtle ligand modifications (electronic, steric) led to dramatic differences in catalytic activity. Generally, a more electron-deficient zinc center would increase the reaction rate due to more efficient CHO coordination, and on the other hand, a decrease of the catalytic activity is expected with a more electron-rich zinc metal center. Coates and co-workers[16] have demonstrated that the addition of an electron-withdrawing cyano group to the β-diimine ligand results in superior activities, giving an 8-fold increase in the copolymerization of CHO/CO_2. Similar trends are observed here, with the addition of an electron-donating allyl or bulky alkane group to the β-diiminate ligand decreasing the catalytic activity. As was shown in Table 1, all the modified zinc complexes had lower activities than the simple BDI zinc complex. In the case of BDI-1-MPTS-based zinc complexes, steric effects also may play a role in the activity decrease and the broader PDI. Nonetheless, all the modified zinc β-diiminate complexes still exhibited good activities in the copolymerization, with excellent carbonate content in the polymer and narrow PDIs.

Silica-supported solid catalysts prepared from each of the three methods were investigated for their performance in the copolymerization of CHO and CO_2. The polymerizations were performed under conditions identical with those for for the homogeneous systems, in neat CHO at 50 °C and with a CO_2 pressure of 100 psi. In several cases, the copolymerization was performed at a higher temperature of 80 °C, but only a slight activity increase was observed. Table 2 summarizes the results from the catalysts supported on SBA-15. A decrease in polymerization activity was observed in these solid catalysts, to about one-sixth the activity of their homogeneous counterparts. Furthermore, there was a reduction in the number of carbonate linkages relative to ether linkages in the resulting polymers compared to the homogeneous systems, with the highest carbonate content being 73% for I−OMe prepared using method 1 and the lowest being 33% for the heterogeneous metalation of III−OMe prepared using method 3. This gradient in copolymer content depending on synthetic procedure may track with the propensity for side reactions to occur during synthesis. Side reactions that cause the partial or complete decomposition of the Zn−BDI complexes would be expected to give zinc species that are either inactive for polymerization or active for the homopolymerization of the epoxide.

The catalytic results also indicate that the methoxy group is a more effective initiating group in the supported catalysts, perhaps because it is less likely to undergo side reactions with the silanols (method 1) or the thiols on the silica surface (method 2) than the amide group. This also could be due to the formation of a different type of immobilized active site upon immobilization of the dimeric methoxy-bridged catalysts compared to the monomeric amide- and ethyl-containing catalysts. Immobilization of the dimeric complexes could lead to two complexes immobilized next to each other on the surface. If the catalytic process required two zinc centers, this could lead to a more active and selective site (vide infra). Alternately, if the presumed anti

(15) Tao, T.; Maciel, G. E. *J. Am. Chem. Soc.* **2000**, *122*, 3118−3126.

(16) Moore, D. R.; Cheng, M.; Lobkovsky, E. B.; Coates, G. W. *Angew. Chem., Int. Ed.* **2002**, *41*, 2599−2602.

Table 2. SBA-15-Supported Catalysts for the Copolymerization of CHO and CO_2[a]

entry	catalyst[b]	Zn loading[c] (mmol/g of silica)	[monomer]/[Cat.]	TON	TOF	carbonate linkages (%)[d]	M_n (kg/mol)	M_w/M_n
1	I−OMe	0.15	1457	72	18	73	15.5	1.31
2	I−$N(SiMe_3)_2$	0.14	2170	60	12	65	21.4	1.40
3	II−OMe	0.14	1467	70	14	61	14.7	1.48
4	II− $N(SiMe_3)_2$	0.12	1680	60	10	43	20.3	1.65
5	III−OMe	0.11	1546	40	5	33	25.2	1.89

[a] All reactions were performed in neat CHO at 50 °C with a constant CO_2 pressure of 100 psi. [b] I−III stand for catalysts prepared by methods 1−3 with appropriate initiating groups, respectively. [c] Zinc complex loading was determined with TGA and was verified by elemental analysis. [d] Calculated by integration of methine resonances in ^1H NMR of the polymer; estimated error is ±1.0%. All catalysts contain the BDI-1 ligand.

Table 3. CPG-Supported Catalysts for the Copolymerization of CHO and CO_2[a]

entry	catalyst[b]	Zn loading[c] (mmol/g of silica)	[monomer]/[Cat.]	TON	TOF	carbonate linkages (%)[d]	M_n (kg/mol)	M_w/M_n
1	I−OMe	0.08	2000	126	21	78	16.6	1.29
2	I−$N(SiMe_3)_2$	0.09	1855	78	13	72	19.7	1.36
3	II−OMe	0.06	2800	102	17	69	15.9	1.40
4	II− $N(SiMe_3)_2$	0.07	2486	54	9	52	17.4	1.55
5	III−OMe	0.05	3400	48	8	41	23.4	1.62

[a] All reactions were performed in neat CHO at 50 °C with a constant CO_2 pressure of 100 psi. [b] I−III stand for catalysts prepared with methods 1−3 with appropriate initiating groups, respectively. [c] Zinc complex loading was determined with TGA and was verified by elemental analysis. [d] Calculated by integration of methine resonances in ^1H NMR of the polymer; estimated error is ±1.0%. All catalysts contain the BDI-1 ligand.

arrangement of the complexes hinders immobilization of both ligands to the surface, it could lead to the covalent immobilization of one complex and the leaching of the other, nonbound complex after activation with CO_2. Method 3 is clearly the least useful method, as the catalyst prepared using this method gave very low rates and poor CO_2 incorporation in the polymer. As mentioned earlier, diethylzinc is unlikely to interact with the silica framework of the silanol-free β-diiminate functionalized SBA-15 or CPG. As (BDI)ZnEt showed no activity in the copolymerization,[9a] the poor performance from III−ZnOMe is more likely due to the difficulty in generating the corresponding zinc methoxide catalysts in situ on the solid support. This transformation is limited by the reaction of methanol with the silica surface, and using a large excess of methanol is not an option, since it leads to demetalation of the ligand.

It is hypothesized that polymer filling of the catalyst pores may limit the kinetics of this system, leading to lower activities and broader PDIs. To probe this, solid catalysts supported on CPG were also evaluated. Due to its larger pore size and interconnected three-dimensional mesoporous structure, CPG should have more efficient mass transport and diffusion. Using CPG, an increase in catalytic activity and a higher percentage of carbonate linkages were observed. However, a major drawback of using CPG as a support is its low surface area, only about 1/10 of that of SBA-15, resulting in low zinc catalyst loading and decreased activity per gram of catalyst. Table 3 lists the copolymerization results from the CPG-supported systems. In all cases, the CPG-supported catalysts showed comparable activities but improved carbonate content in the polymers.

A number of control reactions were undertaken to try and elucidate the cause for the lower CO_2 incorporation in the polymers prepared using supported catalysts. Of course, one possible cause is the potential presence of multiple types of zinc sites on the surface resulting from side reactions during the synthesis. Another possibility is that the copolymerization may require an active center that contains two zinc species, as previous reports indicate that copolymerization is second order with respect to the zinc complex.[16] The fact that supported catalysts based on Zn−amide initiating groups promote the copolymerization with activities and copolymer contents only slightly lower than those of supported catalysts derived from dimeric Zn−OMe catalysts may indicate that a site that is monomolecular in zinc complex may also be able to promote the copolymerization, as it is highly unlikely that the complexes are immobilized in such a manner that allows easy interaction of adjacent surface-bound sites. Certainly, the determination of the nature of the active site both in solution and on supports warrants future investigation.

Another possible cause for lower incorporation of CO_2 in polymers prepared using the supported catalysts may be related to active site accessibility. We hypothesized that the lower carbonate content could be due to starvation of the active site for CO_2, especially during the latter stages of the polymerization when the pores have begun to fill with the polymer. To probe this, the copolymer content was studied both at the early stages of the polymerization and at later points in the process. Using the I−$N(SiMe_3)_2$ catalyst supported on SBA-15, it was found that the carbonate content in the polymer was substantially higher at an early stage (76% after 40 min) than at a later stage of the process (65% after 5 h). This implies that, as the pores fill with polymer, the limiting reactant, CO_2, may be less accessible to the active site, leading to lower carbonate contents. Additional studies were undertaken with the overall pressure of CO_2 modulated to further probe the effect of CO_2 pressure on copolymer content. With the catalyst I−$N(SiMe_3)_2$ supported on SBA-15, no polymerization occurred at a reduced pressure of 50 psi. A pressure of 100 psi appears to be near the lower bound of where the copolymerization will occur. At higher pressures, it was found that the copolymer content increased. For instance, at 600 psi, polymerization with I−$N(SiMe_3)_2$ resulted in a TON of 56, a TOF of 14, and a carbonate content of 74% (60, 12, and 65%, respectively, with a

CO_2 pressure at 100 psi). These results indicate that poor diffusion of CO_2 into the pores of the supported catalyst is one contributing cause for lower carbonate contents in the polymers made via this method. However, the contribution of multiple types of zinc sites caused by side reactions during the supporting process cannot be ruled out, due to the inability to probe the state of the zinc center directly via spectroscopic techniques.

In comparison to other immobilization methods, polymerization studies of the catalysts I−OMe and $-N(SiMe_3)_2$ derived from method 1 indicate that this method is the most likely to give good catalysts with relatively well-defined zinc sites. Useful catalysts were prepared despite the possibility of a side reaction occurring between the weakly Brønsted acidic silanol groups on the surface and the Zn−OMe or Zn−$N(SiMe_3)_2$ groups. The lack of this side reaction occurring in appreciable amounts was hypothesized to be due to steric constraints on the silica surface within the mesopores. To probe whether surface silanols could have detrimental effects on Zn−BDI catalysts, Coates' original $[(BDI)ZnOMe]_2$ was stirred with dry SBA-15 in a toluene suspension at room temperature overnight and the solid was recovered by filtration and washed with hexanes and toluene in a drybox. The filtrate was collected, the solvent was removed, and upon addition of CHO and CO_2, it was determined that the homogeneous catalyst still gave comparable activity (TON = 312, TOF = 156) and the resulting copolymer had good carbonate content (93%). This indicates that extensive contact of the catalyst with mesoporous silica does not significantly deactivate the zinc complex. In addition, the recovered solid SBA-15 was tested for its activity in the copolymerization and no polymer was produced, indicating that essentially no zinc catalyst was physisorbed onto the solid. However, different behavior was observed if a nonporous fumed silica was used as a support. In another experiment, $[(BDI)ZnOMe]_2$ was dissolved in C_6D_6 in an NMR tube and a small amount (~20 mg) of soluble, nonporous, fumed silica (Cab-O-Sil EH-5) was added. ^1H NMR analysis showed that the silica caused complete decomposition of the catalyst, with no methoxy protons visible, only those of the protonated ligand. Furthermore, all attempts to immobilize the BDI-1-based Zn catalysts on the fumed silica support resulted in catalysts that had a very low activity and only traces of homopolymer were formed. These results indicate that the structure of the support is crucial. In SBA-15, the steric constraints at the silica surface imposed by the pore size and shape seem to prevent facile interaction of the zinc center with the surface (concave surface). In contrast, on the nonporous solid with a different, more open radius of curvature on the surface (flat or convex surface), the zinc center can interact with the surface OH groups and decompose the catalyst (see Figure 2). Referring back to the cause of the lower copolymer content in the supported catalysts I−OMe and I−$N(SiMe_3)_2$ compared to their homogeneous analogues, the above results imply that side reactions involving the zinc center and the mesoporous silica surface may not be the primary cause of the lower carbonate content in the polymer. Instead, the primary cause of the lower carbonate content in the polymer

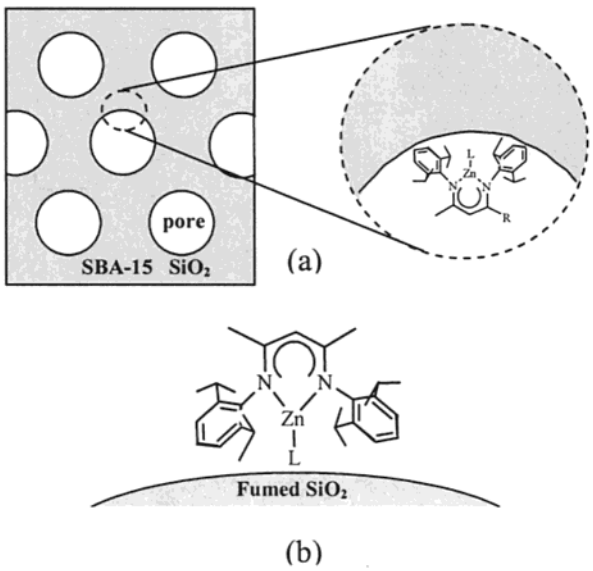

Figure 2. Schematic illustration of the Zn−BDI complex interacting with a silica surface: (a) in mesoporous SBA-15 with unidimensional pores of 105 Å in diameter, where the curvature of the surface could prevent facile interaction of the zinc atom with the silanols of the surface; (b) on a nonporous support such as fumed, colloidal silica, where the relatively flat surface leaves open the possibility of interaction between the silica surface and the zinc center and subsequent decomposition of the Zn−BDI complex.

relative to the homogeneous system could be a lack of CO_2 getting to the active site as mentioned above. In the absence of CO_2, these catalysts do not promote the homopolymerization of the epoxide, either at atmospheric pressure under argon or at 100 psi of argon pressure. Hence, it is unlikely that the reduced carbonate content in the polymers from the heterogeneous catalysts prepared via method 1 are due to homopolymer specific sites; rather, it is more likely that a copolymer is initiated and this growing chain begins to incorporate more ether linkages as the concentration of CO_2 around the active species drops with time.

It is noteworthy that, in both the homogeneous and immobilized catalyst systems, we did not observe cyclic cyclohexene carbonate. This may be attributed to the steric encumbrance provided by the cyclohexene carbonate linkages and the β-diiminate ligand, which inhibit the back-biting mechanism that leads to the formation of cyclic carbonates seen in the reaction between propylene oxide (PPO) and CO_2.[17] Coates[18] recently reported the copolymerization of PPO/CO_2 using unsymmetrical BDI−Zn catalysts with high activity, and we are currently investigating whether immobilized BDI−Zn catalysts will behave differently.

Finally, mechanistic studies by Coates and co-workers suggested that a monomeric zinc β-diiminate species is responsible for the ring-opening polymerization of lactide[19] and β-butyrolactone and β-valerolactone.[20]

(17) (a) Kuran, W.; Listos, T. *Macromol. Chem. Phys.* **1994**, *195*, 997−984. (b) Listos, T.; Kuran, W.; Siwiec, R. *J. Macromol. Sci.-Pure Appl. Chem.* **1995**, *A32*, 393−403. (c) Koinuma, H.; Hirai, H. *Makromol. Chem.* **1977**, *178*, 1283.

(18) Allen, S. D.; Moore, D. R.; Lobkovsky, E. B.; Coates, G. W. *J. Am. Chem. Soc.* **2002**, *124*, 14284−14285.

(19) Chamberlain, B. M.; Cheng, M.; Moore, D. R.; Ovitt, T. M.; Lobkovsky, E. B.; Coates, G. W. *J. Am. Chem. Soc.* **2001**, *123*, 3229−3238.

However, in the copolymerization of CHO and CO_2, it is less clear whether the active species is of a dimeric or a monomeric form.[9a,16] As mentioned above, by immobilizing monomeric zinc amide catalysts on a solid support, we can significantly reduce the likelihood of dimer formation. Because the silica-supported zinc amide catalysts are effective for promoting polycarbonate formation, it is suggested that a monomeric species is capable of promoting CHO and CO_2 copolymerization as well. This conclusion cannot be drawn from simple homogeneous studies, because dimers could always form in situ in solution.

Conclusions

Several new β-diiminate zinc complexes have been prepared and immobilized on silica supports using a variety of synthetic protocols. The reactivity of these mesoporous silica-supported catalysts is influenced by a number of factors, including catalyst preparation methodology, structure of the silica support, and CO_2 pressure. Immobilized catalysts gave moderate polymerization activities compared to their homogeneous analogues, potentially due to pore diffusion effects. The relative compositions of carbonate linkages compared to ether linkages in the produced copolymers have been found to vary with the catalyst preparation procedure, the initiating group, and the CO_2 pressure. The structure of the support was illustrated to have a strong influence on the ability to support the zinc complexes, with mesoporous materials such as SBA-15 and CPG-246 effectively serving as useful supports and nonporous solids such as fumed silica causing complete complex decomposition. The catalysts are currently being evaluated in the ring-opening polymerization of lactide. Future studies concerning polycarbonate synthesis may include a more detailed kinetic study of the initial stages of the process.

Experimental Section

(A) Materials and Instrumentation. All reactions with air- and moisture-sensitive compounds were carried out under a dry nitrogen/argon atmosphere using an MBraun UniLab 2000 drybox and/or standard Schlenk line techniques. Gel permeation chromatography (GPC) analyses were carried out using a Waters instrument equipped with a Waters 410 differential refractometer. The GPC columns (American Polymer Standards) were eluted with THF at a rate of 1 mL/min and were calibrated using 11 polystyrene standards. ^{1}H (300 MHz) and ^{13}C (75 MHz) NMR spectra were recorded on a Mercury VX instrument. Nitrogen physisorption measurements were conducted on a Micromeritics ASAP 2010 system. Samples were pretreated by heating under vacuum at 150 °C for 8 h. A Netzsch Thermoanalyzer STA 409 was used for simultaneous thermal analysis combining thermogravimetric analysis (TGA) and differential scanning calorimetry (DSC) with a heating rate of 10 °C/min in air. FT-Raman spectra were obtained on a Bruker FRA-106 instrument. At least 128 scans were collected for each spectrum, with a resolution of 2−4 cm^{-1}.

CPG with 246 Å pores was purchased (CPG, Inc.). (3-Mercaptopropyl)trimethoxysilane (95%, Gelest), 1,1,1,3,3,3-hexamethyldisilazane (99.9%, Aldrich), 2,6-diisopropylaniline (92%, Acros Organics), zinc bis(bis(trimethylsilyl)amide) (97%, Aldrich), diethylzinc (Alfa-Aaser), and the surfactant Pluronic P123 (M_{av} = 5800, $EO_{20}PO_{70}EO_{20}$, Aldrich) were used as received. Cyclohexene oxide (CHO) was distilled over calcium hydride under vacuum twice and stored in a drybox after three freeze−pump−thaw cycles. Carbon dioxide (Matheson Research Purity Grade, 99.995%) was used as received.

(B) Synthesis of SBA-15 and Thiol-Functionalized SBA-15. SBA-15 was synthesized by literature methods.[11b] The as-prepared material was calcined using the following temperature program: (1) increasing the temperature (1.2 °C/min) to 200 °C, (2) heating at 200 °C for 1 h, (3) increasing the temperature (1.2 °C/min) to 550 °C, and (4) holding at 550 °C for 6 h. The pore size and surface area were measured by low-temperature N_2 physisorption. Prior to functionalization, the SBA-15 was dried under vacuum at room temperature overnight and then at 120 °C for 3 h and stored in a drybox.

Thiol-functionalized SBA-15[21] was synthesized by refluxing a toluene (40 mL) suspension of SBA-15 (1 g) and (3-mercaptopropyl)trimethoxysilane (1 g) for 24 h. The solid was filtered and washed with anhydrous toluene in a drybox and then dried under vacuum at room temperature overnight. TGA showed that 0.372 mmol/g of SiO_2 of the thiol was immobilized on SBA-15. Capping the remaining surface silanols was achieved by stirring the as-synthesized materials with a large excess of hexamethyldisilazane (1.0 g) in toluene (30 mL) at room temperature overnight. The solid was then filtered and washed with toluene in a drybox and dried under vacuum at room temperature overnight.

(C) Synthesis of Ligand Precursors. 1-Allyl-2,4-pentanedione. A modified literature procedure was used.[22] To a suspension of NaH (2.08 g, ca. 46 mmol) in THF (100 mL) was slowly added 2,4-pentanedione (4.30 mL, 42.1 mmol) at 0 °C. After the mixture was stirred for 10 min, *n*-BuLi (1.6 M in hexane, 26.4 mL, 42.2 mmol) was added over a period of 15 min to afford a deep yellow solution of the pentadione dianion. When the mixture was stirred for another 20 min at 0 °C, allyl bromide (3.84 mL, 44.4 mmol) in 5 mL of THF was added dropwise and the yellow color faded. The reaction mixture was then warmed to room temperature and was kept stirring for another 20 min. It was then quenched with concentrated HCl (8 mL in 10 mL H_2O and 30 mL of Et_2O). The organic layer was separated, washed with saturated sodium chloride, and dried over anhydrous $MgSO_4$. Vacuum distillation (20 mTorr, 50 °C) afforded the pure product as a colorless liquid (yield 4.0 g, 72%). ^{1}H NMR ($CDCl_3$; exists mainly in the hydroxyl form): δ 5.80 (1H, m, C*H*═CH_2), 5.02 (2H, t, J = 14.9 Hz, CH═CH_2), 5.49 (1H, s, β-CH), 2.37 (4H, m, −C_2H_4−), 2.05 (3H, s, Me) ppm. Mass (FAB): M^+ m/z 140.

4-Allyl-2,6-diisopropylaniline. This synthesis was based on a literature preparation of 4-allyl-2,6-xylidine.[23] Allyl chloride (2.90 g, 37.89 mmol) and 2,6-diisopropylaniline (8.20 g, 42.55 mmol) were mixed in xylene (20 mL) and heated to 120 °C overnight. After it was cooled to room temperature, the mixture was stirred with 20% NaOH (10 mL), washed with saturated NaCl (3 × 12 mL), and then dried by distilling off the xylene. Fractional distillation (70 °C, 20 mTorr) afforded the pure *N*-allyl-2,6-diisopropylaniline as a colorless liquid. ^{1}H NMR ($CDCl_3$): δ 7.05 (2H, d, J = 7.5 Hz, Ar H), 6.82 (1H, t, J = 7.7 Hz, Ar H), 6.05 (1H, m, C*H*═CH_2), 5.33 (1H, m, J = 17.1 Hz, CH═C*H*H′), 5.17 (1H, m, J = 9.9 Hz, CH═CH*H*′), 3.75 (1H, b, NH), 3.52 (2H, m, J = 5.2 Hz, CH_2), 2.94 (2H, hept, J = 6.9 Hz, C*H*Me_2), 1.25 (12H, d, J = 7.2 Hz, CH*Me*$_2$) ppm.

N-Allyl-2,6-diisopropylaniline (7.02 g, 32.31 mmol) and $ZnCl_2$ (4.86 g, 35.74 mmol) were mixed in 20 mL of xylene and heated to reflux for 4 h to effect an aza-Claisen rearrangement.

(20) Rieth, L. R.; Moore, D. R.; Lobkovsky, E. B.; Coates, G. W. *J. Am. Chem. Soc.* **2002**, *124*, 15239−15248.

(21) Yiu, H. H. P.; Wright, P. A.; Botting, N. P. *J. Mol. Catal. B* **2001**, *15*, 81−92.

(22) Stuart, N. H.; Weiler, L. *J. Am. Chem. Soc.* **1974**, *96*, 1082−1087.

(23) Elliott, M.; Janes, N. F. *J. Chem. Soc. C* **1967**, 1780−1782.

Next, the mixture was cooled to room temperature and then stirred with NaOH (5.4 g in 20 mL of H_2O). The organic layer was extracted with ether, washed with saturated NaCl, and dried over anhydrous $MgSO_4$. The pure 4-allyl-2,6-diisopropylaniline was separated from the unreacted *N*-allyl complex through fractional distillation (80 °C, 20 mTorr) as a colorless liquid. Yield: 3.30 g (47%). ^{1}H NMR ($CDCl_3$): δ 6.84 (2H, s, Ar H), 5.96 (1H, m, C*H*═CH_2), 5.03 (2H, t, J = 15.45 Hz, CH═C*H*$_2$), 3.62 (2H, b, NH), 3.30 (2H, d, J = 7.2 Hz, CH_2), 2.90 (2H, septet, J = 6.9 Hz, C*H*Me_2), 1.25 (12H, d, J = 7.2 Hz, CH*Me*$_2$) ppm.

(D) Ligand Synthesis. (BDI-1)H and (BDI-2)H were synthesized using a reported procedure with some modification.[24]

(BDI-1)H. 2,6-Diisopropylaniline (9.0 g, 46.71 mmol) and 1-allyl-2,4-pentanedione (3.0 g, 21.43 mmol) were dissolved in absolute ethanol (50 mL). Anhydrous sodium sulfate (1.0 g) was used as water adsorbent, and concentrated hydrochloric acid (1.8 mL, 22.3 mmol) was added via syringe. The mixture was refluxed for 3 days. The solvent was then evaporated to afford a light brown solid. The solid was washed with hexanes to leave a cream-colored solid, which was suspended in CH_2Cl_2 and neutralized with saturated sodium carbonate (80 mL). The organic collection was passed through a short silica gel column, and the solvent was removed under vacuo. Excess 2,6-diisopropylaniline was distilled off under vacuum (90 °C, 20 mTorr), leaving the pure (BDI-1)H as a viscous light yellow liquid. Yield: 4.5 g (46%). ^{1}H NMR ($CDCl_3$): δ 12.10 (1H, b, NH), 7.10 (6H, m, Ar H), 5.71(1H, m, C*H*═CH_2), 4.96 (1H, m, CH═C*H*H′), 4.90 (1H, m, CH═CH*H*′), 4.87 (1H, s, β-CH), 3.07 (4H, septet, J = 6.4 Hz, C*H*Me_2), 2.22 (2H, m, CH_2CH_2), 2.05 (2H, m, CH_2CH_2), 1.71 (3H, s, α-Me), 1.19 (12H, dd, J = 6.6 Hz, J = 3.7 Hz, CH*Me*Me′), 1.09 (12H, dd, J = 7.2 Hz, J = 3.5 Hz, CHMe*Me*′) ppm. ^{13}C{^{1}H} NMR ($CDCl_3$): δ 163.28, 162.25, 146.46, 143.09, 142.09, 139.54, 137.09, 125.49, 124.97, 123.73, 123.18, 115.11, 91.77, 41.50, 32.67, 28.48, 25.02, 24.60, 23.72, 23.35, 21.53 ppm. Anal. Calcd for $C_{32}H_{46}N_2$: C, 83.79; H, 10.11; N, 6.11. Found: C, 83.84; H, 10.15; N, 5.95.

(BDI-2)H. This ligand was prepared in a manner analogous to that described for (BDI-1)H, by simply using 4-allyl-2,6-diisopropylaniline (1.70 g, 7.83 mmol) and 2,4-pentanedione (0.39 g, 3.90 mmol). Yield: 0.74 g (38%). ^{1}H NMR ($CDCl_3$): δ 12.07 (1H, b, NH), 6.90 (4H, m, Ar H), 5.97 (2H, m, C*H*═CH_2), 5.05 (4H, m, CH═CH_2), 4.82 (1H, s, β-CH), 3.34 (4H, d, J = 6.6 Hz, −CH_2−), 3.05 (4H, septet, J = 6.9 Hz, C*H*Me_2), 1.69 (6H, s, α-Me), 1.17 (12H, d, J = 7.2 Hz, CH*Me*Me′), 1.08 (12H, d, J = 7.2 Hz, CHMe*Me*′) ppm. ^{13}C{^{1}H} NMR ($CDCl_3$): δ 161.43, 142.43, 138.87, 138.11, 136.51, 123.36, 115.62, 93.31, 40.65, 28.57, 24.60, 23.62, 21.13 ppm. Anal. Calcd for $C_{35}H_{50}N_2$: C, 84.28; H, 10.10; N, 5.62. Found: C, 84.24; H, 10.23; N, 5.59.

(BDI-1-MPTS)H. (BDI-1)H (1.0 g, 2.18 mmol), (3-mercaptopropyl)trimethoxysilane (MPTS; 1.3 g, 6.57 mmol), and AIBN (40 mg) were dissolved in chloroform (30 mL), and the solution was refluxed overnight. After the mixture was cooled to room temperature, chloroform was removed and excess MPTS was distilled off under vacuum (90 °C, 20 mTorr) to afford pure product as a light yellow viscous liquid. Yield: 1.36 g (100%). ^{1}H NMR ($CDCl_3$): δ 12.09 (1H, b, NH), 7.09 (6H, m, Ar H), 4.86 (1H, s, β-CH), 3.54 (9H, s, OMe), 3.07 (4H, septet, J = 4.5 Hz, C*H*Me_2), 2.44 (4H, m, J = 6.9 Hz, CH_2SCH_2), 1.97 (2H, t, J = 8.7 Hz, CH_2), 1.71 (3H, s, α-Me), 1.65 (2H, m, CH_2), 1.56 (2H, m, CH_2), 1.47 (2H, m, CH_2), 1.19 (12H, dd, J = 6.6 Hz, J = 3.9 Hz, CH*Me*Me′), 1.08 (12H, dd, J = 6.6 Hz, J = 4.5 Hz, CHMe*Me*′), 0.72 (2H, t, J = 8.3 Hz, CH_2Si) ppm. ^{13}C{^{1}H} NMR ($CDCl_3$): δ 163.58, 162.25, 143.09, 142.06, 139.54, 125.46, 124.91, 123.70, 123.15, 91.77, 50.85, 42.02, 35.31, 32.97, 32.03, 30.03, 28.54, 27.05, 25.02, 24.56, 23.72, 23.32, 21.50, 8.99 ppm.

(E) Zinc Complex Syntheses. (BDI-1)ZnEt. To a solution of diethylzinc (0.760 g, 6.18 mmol) in toluene (10 mL) was slowly added (BDI-1)H (0.52 g, 1.14 mmol) in toluene (5 mL) at 0 °C. After being stirred overnight at 80 °C, the clear yellow solution was cooled to room temperature and the solvent was removed under vacuum, giving the product as a colorless solid in a quantitative yield. ^{1}H NMR (C_6D_6): δ 7.10 (6H, m, Ar H), 5.51 (1H, m, C*H*═CH_2), 5.08 (1H, s, β-CH), 4.83 (2H, m, J = 13.0 Hz, CH═CH_2), 3.20 (4H, septet, J = 6.0 Hz, C*H*Me_2), 2.25 (4H, m, CH_2), 1.75 (3H, s, α-Me), 1.28 (6H, d, J = 5.7 Hz, Me), 1.26 (6H, d, J = 5.7 Hz, Me), 1.20 (6H, d, J = 6.6 Hz, Me), 1.15 (6H, d, J = 6.6 Hz, Me), 0.90 (3H, t, J = 8.1 Hz, CH_2CH_3), 0.26 (2H, q, J = 7.8 Hz, CH_2CH_3) ppm.

[(BDI-1)Zn(μ-OMe)]$_2$. To a solution of (BDI-1)ZnEt (0.628 g, 1.14 mmol) in toluene (10 mL) was added methanol (40 mg, 1.25 mmol) at room temperature. After the mixture was stirred for 2 h, the solvent was removed to afford the product as a pale yellow oily solid in quantitative yield. ^{1}H NMR (C_6D_6): δ 7.12 (6H, m, Ar H), 5.40 (1H, m, C*H*═CH_2), 4.86 (1H, s, β-CH), 4.79 (2H, m, J = 15.3 Hz, CH═CH_2), 3.42 (3H, s, OMe), 2.95 (4H, m, C*H*Me_2), 2.16 (2H, m, CH_2), 2.07 (2H, m, CH_2), 1.56 (3H, s, α-Me), 1.19 (24H, m, CH*Me*$_2$) ppm. Anal. Calcd for $C_{33}H_{48}N_2OZn$: C, 71.53; H, 8.73; N, 5.06. Found: C, 71.44; H, 8.82; N, 4.95.

(BDI-1)ZnN(SiMe$_3$)$_2$. To a solution of (BDI-1)H (0. 60 g, 1.31 mmol) in toluene (10 mL) was added $Zn[N(SiMe_3)_2]_2$ (0.505 g, 1.31 mmol), and the solution was stirred for 6 days at 80 °C. After removal of solvent under vacuum and recrystallization from toluene at −30 °C, a yellow oily solid was recovered. Yield: 0.565 g (63%). ^{1}H NMR (C_6D_6): δ 7.11 (6H, m, Ar H), 5.48 (1H, m, C*H*═CH_2), 4.94 (1H, s, β-CH), 4.80 (2H, m, J = 10.7 Hz, CH═CH_2), 3.27 (4H, septet, J = 7.1 Hz, C*H*Me_2), 2.15 (4H, m, CH_2), 1.68 (3H, s, Me), 1.21 (6H, d, J = 7.2 Hz, CH*Me*Me′), 1.17 (6H, d, J = 6.9 Hz, CHMe*Me*′), 1.14 (6H, d, J = 2.1 Hz, CH*Me*″Me‴), 1.11 (6H, d, J = 2.7 Hz, CHMe″*Me*‴), 0.19 (18H, s, Si*Me*) ppm. Anal. Calcd for $C_{38}H_{63}N_3Si_2Zn$: C, 66.78; H, 9.29; N, 6.15. Found: C, 66.67; H, 9.23; N, 6.07.

[(BDI-1)Zn(μ-O^{i}Pr)]$_2$. To a solution of (BDI-1)ZnN(SiMe$_3$)$_2$ (0.44 g, 0.64 mmol) in toluene (10 mL) was added 2-propanol (40 mg, 0.66 mmol), and the mixture was stirred overnight at room temperature. Removal of solvent and recrystallization from toluene at −30 °C afforded the product as a light yellow oily solid. Yield: 0.217 g (58%). ^{1}H NMR (C_6D_6): δ 7.15 (6H, m, Ar H), 5.54 (1H, m, C*H*═CH_2), 4.96 (1H, s, β-CH), 4.83 (2H, m, CH═CH_2), 3.63 (1H, m, J = 4.2 Hz, OC*H*Me_2), 3.31 (4H, septet, J = 7.2 Hz, C*H*Me_2), 2.18 (4H, m, CH_2), 1.71 (3H, s, α-Me), 1.24 (6H, d, J = 6.6 Hz, CH*Me*Me′), 1.20 (6H, d, J = 6.6 Hz, CHMe*Me*′), 1.17 (6H, d, J = 2.7 Hz, CH*Me*″Me‴), 1.14 (6H, d, J = 2.4 Hz, CHMe″*Me*‴), 0.93 (6H, d, J = 6.3 Hz, OCH*Me*$_2$) ppm.

Similar procedures were followed to synthesize the corresponding BDI-2-based and BDI-1-MPTS-based complexes.

(BDI-2)ZnEt. ^{1}H NMR (C_6D_6): δ 7.14 (2H, s, Ar H), 6.96 (2H, s, Ar H), 6.03 (2H, m, C*H*═CH_2), 5.04 (4H, m, CH═CH_2), 5.02 (1H, s, β-CH), 3.37 (4H, d, J = 6.6 Hz, CH_2), 3.00 (4H, septet, J = 7.5 Hz, C*H*Me_2), 1.75 (6H, s, α-Me), 1.22 (12H, m, J = 3.7 Hz, CH*Me*Me′), 1.11 (12H, m, J = 3.7 Hz, CHMe*Me*′), 0.42 (3H, t, J = 8.4 Hz, CH_2CH_3), −0.29 (2H, q, J = 8.1 Hz, CH_2CH_3) ppm.

[(BDI-2)Zn(μ-OMe)]$_2$. ^{1}H NMR (C_6D_6): δ 7.09 (2H, s, Ar H), 6.92 (2H, s, Ar H′), 6.00 (1H, m, C*H*═CH_2), 5.32 (1H, s, β-CH), 5.06 (2H, t, J = 14.9 Hz, CH═CH_2), 3.67 (3H, s, O*Me*), 3.34 (4H, d, J = 6.6 Hz, CH_2), 2.84 (4H, septet, J = 6.9 Hz, C*H*Me_2), 1.79 (6H, s, α-CH_3), 1.11 (24H, m, CH*Me*$_2$) ppm. Anal. Calcd for $C_{36}H_{52}N_2OZn$: C, 72.77; H, 8.82; N, 4.71. Found: C, 72.71; H, 8.77; N, 4.65.

[(BDI-2)Zn(μ-O^{i}Pr)]$_2$. ^{1}H NMR (C_6D_6): δ 7.07 (4H, s, Ar H), 5.98 (2H, m, C*H*═CH_2), 5.04 (4H, m, J = 16.8 Hz, CH═CH_2), 4.86 (1H, s, β-CH), 3.44 (1H, m, OC*H*Me_2), 3.30 (4H, m,

(24) Feldman, J.; McLain, S. J.; Parthasaranthy, A.; Marshall, W. J.; Calabrese, J. C.; Arthur, S. D. *Organometallics* **1997**, *16*, 1514−1516.

C*H*Me$_2$), 2.07 (4H, s, CH$_2$), 1.66 (6H, s, α-Me), 1.20 (12H, d, J = 7.2 Hz, CH*Me*Me′), 1.15 (12H, d, J = 6.6 Hz, CHMe*Me*′), 0.85 (6H, m, J = 6.5 Hz, OCH*Me*$_2$) ppm.

(BDI-2)ZnN(SiMe$_3$)$_2$. ^{1}H NMR (C$_6$D$_6$): δ 7.12 (2H, s, Ar H), 7.10 (2H, s, Ar H′), 6.00 (2H, m, C*H*═CH$_2$), 5.06 (4H, m, J = 11.7 Hz, CH═C*H*$_2$), 4.89 (1H, s, β-CH), 3.31 (8H, m, C*H*Me$_2$ +C*H*$_2$), 1.69 (6H, s, α-Me), 1.20 (24H, m, CH*Me*$_2$), 0.09 (9H, s, SiMe$_3$), 0.01 (9H, s, SiMe′$_3$) ppm.

(BDI-1-MPTS)ZnEt. ^{1}H NMR (CD$_2$Cl$_2$): δ 7.14 (6H, m, Ar H), 5.03 (1H, s, β-CH), 3.52 (9H, s, OMe), 3.01 (4H, septet, J = 6.6 Hz, C*H*Me$_2$), 2.42 (4H, pentet, J = 6.9 Hz, C*H*$_2$SC*H*$_2$), 2.05 (2H, t, J = 8.0 Hz, CH$_2$), 1.77 (3H, s, α-Me), 1.61 (4H, m, CH$_2$), 1.47 (2H, m, CH$_2$), 1.22 (12H, d, J = 6.6 Hz, CH*Me*Me′), 1.11 (12H, dd, J = 7.2, 2.7 Hz, CHMe*Me*′), 0.69 (2H, t, J = 8.3 Hz, C*H*$_2$Si), 0.37 (3H, t, J = 8.3 Hz, CH$_2$*Me*), −0.32 (2H, q, J = 8.1 Hz, C*H*$_2$Me) ppm.

[(BDI-1-MPTS)Zn(μ-OMe)]$_2$. ^{1}H NMR (C$_6$D$_6$): δ 7.08 (6H, m, Ar H), 4.98 (1H, s, β-CH), 3.45 (3H, s, OMe), 3.38 (9H, s, OMe), 3.00 (4H, m, J = 6.6 Hz, C*H*Me$_2$), 2.73 (2H, m, J = 7.2 Hz, CH$_2$), 2.43 (2H, t, J = 7.4 Hz, CH$_2$), 2.30 (2H, t, J = 7.2 Hz, SC*H*$_2$), 2.17 (2H, t, J = 6.9 Hz, C*H*$_2$S), 2.06 (2H, t, J = 8.6 Hz, CH$_2$), 1.73 (2H, t, J = 9.5 Hz, CH$_2$), 1.58 (3H, s, Me), 1.22−1.13 (24H, m, CH*Me*$_2$), 0.72 (2H, t, J = 8.3 Hz, C*H*$_2$Si) ppm. Anal. Calcd for $C_{39}H_{64}N_2O_4SSiZn$: C, 62.42; H, 8.60; N, 3.73; S, 4.27. Found: C, 62.34; H, 8.53; N, 3.69; S, 4.18.

(BDI-1-MPTS)ZnN(SiMe$_3$)$_2$. ^{1}H NMR (C$_6$D$_6$): δ 7.13 (6H, m, Ar H), 4.99 (1H, s, β-CH), 3.38 (9H, s, OMe), 3.29 (4H, m, J = 6.6 Hz, C*H*Me$_2$), 2.44 (2H, t, J = 7.5 Hz, CH$_2$), 2.29 (2H, t, J = 7.2 Hz, CH$_2$), (4H, m, C*H*$_2$SC*H*$_2$), 2.06 (2H, m, CH$_2$), 1.81 (2H, m, J = 7.6 Hz, CH$_2$), 1.32 (3H, s, Me), 1.26−1.11 (24H, m, CH*Me*$_2$), 0.77 (2H, t, J = 8.9 Hz, C*H*$_2$Si), 0.19 (18H, s, Si*Me*$_3$) ppm. Anal. Calcd for $C_{44}H_{79}N_3O_3SSi_3Zn$: C, 60.07; H, 9.05; N, 4.78; S, 3.64. Found: C, 59.91; H, 8.93; N, 4.62; S, 3.47.

(F) Immobilization of Zinc Catalysts on a Silica Surface. With each method, the resulting solid catalysts were dried under vacuum at room temperature overnight and characterized by FT-Raman spectroscopy. The catalyst loading was determined by TGA and elemental analysis.

Method 1. In a typical preparation, [(BDI-1-MPTS)ZnOMe]$_2$ (100 mg, 0.268 mmol) was added into a toluene suspension (30 mL) of dry SBA-15 (400 mg) or CPG-246 (500 mg), and the mixture was stirred for 24 h at room temperature. The solid catalyst was collected by filtration and washed with anhydrous toluene and dry hexanes in a drybox.

Method 2. (BDI-1)ZnN(SiMe$_3$)$_2$ (150 mg, 0.170 mmol), AIBN (40 mg), and thiol-functionalized SBA-15 (400 mg) or CPG-(246) (700 mg) were mixed in chloroform (30 mL). The mixture was refluxed overnight. After it was cooled to room temperature, it was filtered and washed with hexanes and toluene in a drybox.

Method 3. (BDI-1-MPTS)H (346 mg, 0.755 mmol) was added to a toluene (30 mL) suspension of SBA-15 (600 mg) or CPG-240 (1.0 g) and was stirred for 24 h at room temperature. It was then filtered and washed with toluene to afford the β-diimine ligand functionalized SBA-15 or CPG. Metalation was carried out by adding a 5 equiv excess of ZnEt$_2$ or 1 equiv of Zn(N(SiMe$_3$)$_2$)$_2$ based on the loading of the BDI-MPTS ligand on the solid, typically in 40 mL of toluene. The metalation for diethylzinc was achieved at 80 °C for 24 h, with a reaction time of 1 week for the zinc amide. The resulting solid catalysts were collected by filtration and washed with toluene in a drybox. The former was then stirred in toluene with 5 equiv of methanol in toluene for 24 h and then filtered and dried.

(G) General Polymerization Procedure. In a drybox, the desired zinc complex (3.0×10^{-5} mol) and cyclohexene oxide (3.0 g, 30.6 mmol) were placed in a 60 mL Fischer-Porter bottle with a magnetic stir bar. The vessel was pressurized to 100 psi with CO$_2$, and the mixture was stirred at the desired temperature for the necessary reaction time. After reaction, a small sample of the crude mixture was removed for NMR analysis, the product was dissolved in minimal methylene chloride, and the polymer was precipitated with methanol, which was centrifuged and dried under vacuum to constant weight.

In a similar preparation, the solid catalysts (120∼200 mg) and cyclohexene oxide (3.0 g, 30.6 mmol) were placed into a Fischer-Porter bottle and pressurized with 100 psi of CO$_2$. A small sample of the crude mixture was removed after the necessary reaction time at a given temperature, and the product was precipitated with 20 mL of methanol and centrifuged. The crude sample was dissolved in deuterated chloroform and passed through a small alumina plug before NMR analysis. The rest of the polymer was separated from the silica support by passing through a short alumina column and eluted with large amount of methylene chloride, and the solution was concentrated and precipitated with methanol again. The polymer was then obtained via centrifugation and dried under vacuum to constant weight.

For polymerizations at pressures greater than 100 psi, a 25 mL stainless steel stirred Parr 4590 micro autoclave was utilized. The reactor was loaded with catalyst and CHO in a drybox as described above, removed from the box, and connected to a CO$_2$ cyclinder via a "quick-connect" Swagelock fitting. The reactor was heated to 50 °C using the associated Parr 4843 controller.

Acknowledgment. The National Science Foundation is gratefully acknowledged for partial support of this work (Grant No. CTS-0210460). C.W.J. thanks the Shell Oil Company Foundation and Oak Ridge Associated Universities for partial support of this work through a Faculty Career Initiation Award and a Ralph Powe Junior Faculty Award, respectively.

OM030209W